Surface Science 197 (1988) 474–508
North-Holland, Amsterdam

SURFACE CHEMISTRY OF TRANSITION METAL CARBIDES: A THEORETICAL ANALYSIS

Susan A. JANSEN and Roald HOFFMANN

Department of Chemistry and Materials Science Center, Cornell University, Ithaca, NY 14853, USA

Received 17 April 1987; accepted for publication 18 August 1987

Extended Hückel tight binding calculations have been employed to analyze the interactions of oxygen, carbon monoxide and methanol with the (100) and (111) faces of a representative rocksalt carbide, TiC. The (111) face has been experimentally shown to be the most active toward the adsorption, dissociation or decomposition of adsorbates, whereas the (100) face demonstrates very little activity. Our calculations suggest that the differential reactivity of the two faces is the result of the coordination of the atom in the active site and the presence of surface carbon. For CO on the (100) face the population of the $2\pi^*$ level increases if carbon vacancies are included in the calculations and dissociation occurs. For the (111) metal-terminated face of TiC the population of the $2\pi^*$ level is nearly identical to that calculated for Ti(0001). Methanol dissociates into methoxy and a protic species on the (111) face but remains molecular on the (100). The calculations suggest that the molecular species is stabilized by interaction of the methanolic proton with the surface carbon.

1. Introduction

The initial steps in the development of modern surface chemistry and applications to catalysis have dealt with clean metal and alloy surfaces. A natural evolution of such studies is to consider the effect of surface contamination on chemisorption and catalysis. It is within this framework that recent experimental investigations have focused on sulfur, oxygen and potassium coadsorbates, which may poison or promote the surface in ways which are beginning to be understood [1].

Many surface reactions of interest involve organic molecules. There is ample evidence that in most such reactions the molecules are decomposed, leaving not only CH_x fragments but carbon on the surface. There are persistent hints that the true catalytic activity of metal surfaces may depend critically on the initial formation of carbon overlayers, or *carburized surfaces*.

One wishes to know more about the structure of these active sites. Where is the carbon on the surface? Does it penetrate into the bulk? What is the state of aggregation of the surface carbon? These questions are being actively studied. One obvious approach (whose relevancy to the activity of carburized surfaces

0039-6028/88/$03.50

remains to be determined) is to focus on the reactivity of *carbide* surfaces. These are the surfaces of real bulk transition metal carbides.

Transition metal carbides have extraordinary physical properties. They are extremely hard, yet good conductors of electricity. Their structures are sometimes simple (TiC, WC), sometimes complicated (Fe_3C, Fe_5C_2) [2]. The bonding in these bulk carbides is being explored by theoreticians [3]. It has become possible to prepare metal carbide surfaces which resemble at the exposed surface the structure one might imagine for a clean metal surface with carbon chemisorbed. Recent investigation of the reaction of transition metal carbides and carburized surfaces have suggested that the presence of carbon at the surface may catalyze certain reactions while poisoning others [4]. Theoretical studies into the electronic properties of the surface and adsorbate–surface interactions may suggest a rationale for the various reactivities of the carbide surfaces, and this is our reason for undertaking them.

2. Experimental studies on carbides, especially TiC

There have been numerous studies of the catalytic activity of polycrystalline carbides [5]. For instance, the relative reactivity of carbides with respect to *cis–trans* isomerization has been evaluated as:

$$TiC < ZrC < VC < Cr_2C_3 < HfC < NbC < TaC < WC, \quad (1)$$

and for ammonia oxidation, as:

$$TiC < VC < WC < Mo_2C < ZrC < Cr_2C_3. \quad (2)$$

General comparisons with polycrystalline metals indicate that the gross activity of carbides is not high [6]. The activity of certain prepared surfaces may still be substantial.

We have chosen for specific theoretical investigation TiC, in part because its structure is simple, in part because the catalytic activity of the corresponding free metal is high, but mainly because the (100) and (111) faces of TiC and NbC have been investigated thoroughly with respect to the adsorption of O_2, CO and CH_3OH [7–10].

First a few words about the structure of the bulk material. Most transition metal carbides crystallize into simple structures such as the rock salt, nickel arsenide or hexagonally closest packed structures. A few of these transition metal carbides crystallize into several crystalline phases depending on the metal to carbon ratio. TiC and NbC possess the NaCl structure, two interpenetrating metal and carbon face-centered-cubic lattices. Each metal is octahedrally coordinated by six carbons, each carbon by an octahedron of six metals. A view of the bulk structure is given in scheme 1 and a schematic of the unreconstructed (100) and (111) surfaces in schemes 2 and 3 (○: M, ●: C).

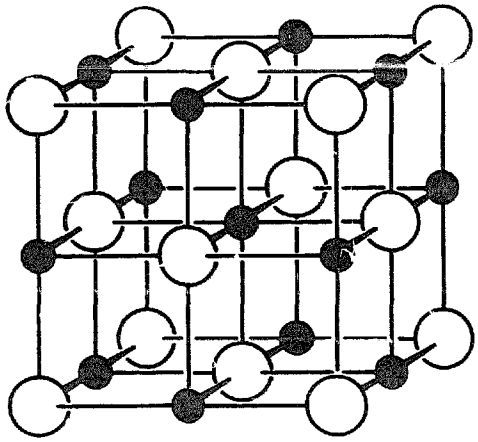

Scheme 1.

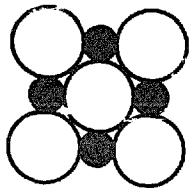
Scheme 2.

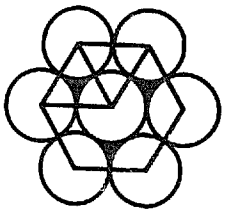
Scheme 3.

Note that for the (111) surface, there are alternative faces with the same indices, but exposing metal or carbon atoms. The representation shown is for the metal-rich face.

Titanium metal is known to adsorb oxygen dissociatively. In studies on titanium metal, the adsorption of oxygen occurs with significant oxygen penetration into the bulk [6]. One impetus for studying the oxidation of TiC is that the reactivity of the (111) face demonstrates behavior similar to that of Ti metal, though penetration of the oxygen atoms into the bulk of the carbide has not been observed, suggesting that the carbide may be more resistant to oxidation than titanium metal. Because of the reduced activity of TiC with respect to oxidation, TiC has been proposed as a coating for certain steel alloys [11].

The adsorption of oxygen on TiC is exclusively dissociative. Several studies on adsorption of atomic oxygen on TiC have provided insight not only into the surface adsorption of oxygen but into the overall reactivity of TiC surfaces. The adsorption of oxygen was studied experimentally on two crystal faces: (111) and (100). On the most common crystal faces, the activity appears to be related to the number of metal–carbon linkages broken as the surface is cleaved:

$$(111) > (110) > (100).$$

Actually, attempts at preparation of the (110) face provided only faceted surfaces, and hence this face was not considered in the experimental studies. For the adsorption of oxygen atoms, the (111) face was 100 times more reactive than the (100). These two faces are considered below in our theoretical analysis, as they demonstrate the extremes in the reactivity of this material [12].

Table 1
Surface dipole moments of representative systems

Substrate material + O	Electronegativity	Percentage ionic character	Surface dipole moment (D)
C	2.5	22	0.11
Ti	1.5	63	0.44
Cu	1.9	47	–
Ag	1.9	47	0.54
W	1.7	56	0.44
TiC			0.17

The adsorption sites of atomic oxygen are reasonably well known for both the (111) and (100) surfaces of TiC. The (111) face is composed entirely of metal or carbon atoms. The surface analyzed is that in which the top layer is composed of titanium. This provides, in principle, for the following adsorption sites: (a) metal threefold hollow, (b) metal twofold bridging, (c) metal on top, all illustrated in scheme 4. From UPS measurements, two adsorption sites have been observed for this surface. One site is the threefold metal hollow. The other adsorption site has not yet been structurally characterized, but is believed to be a bridging site [13].

The (100) surface shows the greatest diversity in adsorption site as both carbon and titanium atoms are implicated in potential adsorption sites. Surface dipole moment studies on oxygenated surfaces have implied predominant bonding to carbon in the most reactive adsorption sites. The experimental results are summarized in table 1 [8,14].

From this table, and a comparison of the surface dipole moments, it is possible to assess the contribution of titanium–oxygen and carbon–oxygen interaction to the total surface dipole. The rationale is as follows: for oxygen on a graphite surface the dipole moment is estimated 0.11 D, for a titanium surface with adsorbed oxygen the dipole moment is extrapolated to be 0.44 D. The following relationship suggests the average percentage carbon and titanium character for the TiC(100) face:

$$0.17\ \mathrm{D(TiC-O)} = [(0.11\ \mathrm{D})(x)\mathrm{C} + (0.44\ \mathrm{D})(1-x)\mathrm{Ti}]\{100\}. \quad (3)$$

It follows from this model that the percentage of oxygenated carbon is about 81% and that of titanium is about 19%.

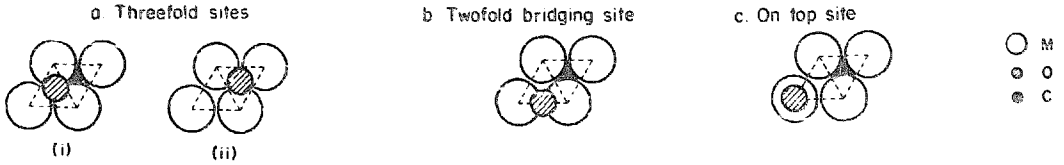

Scheme 4.

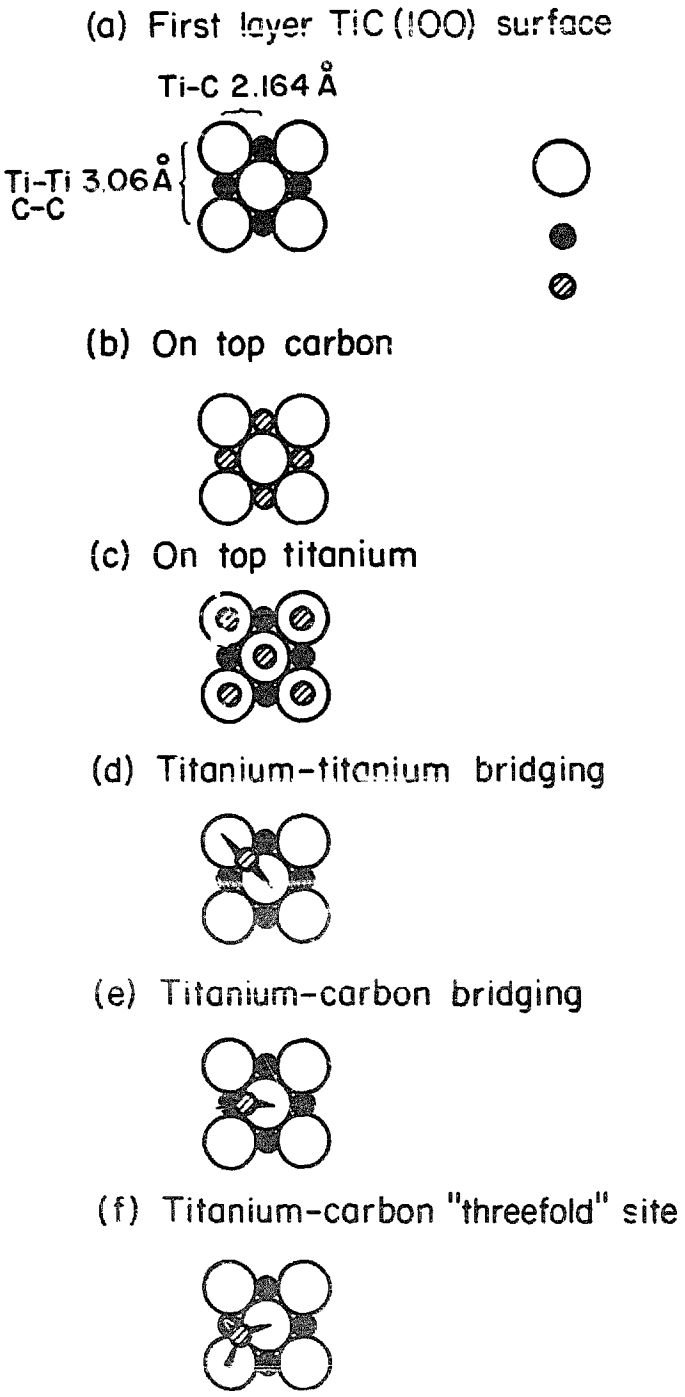

Fig. 1. Possible adsorption sites for oxygen on TiC(100).

Experimental measurements have suggested adsorption sites which are consistent with the dipole moment measurements. Ion scattering spectroscopy (ISS) has been used to characterize the (100) face of TiC. This technique involves bombarding the surface with helium or other inert gas ions and

measuring the trajectory and energy after collision with the surface. The trajectory will give and indication of the surface structure, while the energy will be representative of the incident surface atom. The sampling depth of this technique is ~ 10 Å. There are five likely sites for adsorption on the (100) face. These are shown in fig. 1.

The ISS experimental data suggest that sites a, b and c are those most favorable. From the spectral measurements, it is concluded that as the dosage of oxygen is increased there is a corresponding loss of intensity in the carbon 1s peak, until it is no longer within the limit of detection. This suggests preferential adsorption at carbon-rich sites. Some loss of intensity is also observed in the Ti 2p peaks, suggesting that Ti may be involved in adsorption but to a lesser extent than was the carbon [8].

There is also a good bit of experimental work on NbC surfaces. The structure of NbC is very similar to that of TiC, and this similarity is reflected in the observed properties of the surface.

Studies on the adsorption of O_2, CO and CH_3OH on the (111) and (100) faces of NbC have suggested that the activity of this material is similar to that of TiC [11,15]. The studies of oxygen adsorption on these two surfaces parallel those on TiC. The adsorption of CO on the (111) face of NbC occurs dissociatively while both molecular and dissociative states are observed on the (100) face, though the concentration of molecular CO is significantly greater. The dissociative states of CO on the (100) face are suspected to be due to carbon vacancies or defects at the surface. The "deactivation" of this surface is believed to be due to the presence of exposed carbon at the surface. UPS studies of methanol on these two surfaces show that methanol remains molecular on the (100) surface. On the (111) face, methoxy is detected. The UPS experiments indicate that the main interaction in both cases is with the oxygen lone pairs of the methanolic species, suggesting that the methanolic C–O bond vector may be nearly perpendicular to the surface plane. This is

Table 2
Parameters used in calculations (from ref. [18])

Element	χ_μ	ζ_μ	$H_{\mu\mu}$ (eV)
Ti	4s	1.50	−6.3
	4p	1.50	−3.2
	3d	4.55 $c_1 = 0.4206$	−5.9
		$c_2 = 0.7839$	
C	2s	1.625	−18.2
	2p	1.625	−9.5
O	2s	2.275	−29.6
	2p	2.275	−13.6
H [a]	1s	1.30	−12.2

[a] This value was obtained through charge interaction for bridging H on TiC(100) while keeping the other $H_{\mu\mu}$'s constant.

consistent with the orientation of methanol on other transition metal surfaces.

For methanol on the (100) surface the oxygen is suspected to interact almost exclusively with the surface carbon. For the (111) face, the oxygen lone-pair orbitals interact with surface titanium atoms. The oxygen of the methoxy species is believed to sit in either a threefold or twofold site. On Ni(111), the oxygen of the methanol is thought to sit in a twofold site [16]. Methoxy is believed to adopt adsorption sites and interact with surface atoms in a manner similar to atomic oxygen. For atomic oxygen on surfaces in which the surface bonds are long, i.e. nonclosest packed surfaces, the oxygen seems to prefer a bridging site. This is observed for oxygen on nickel and tungsten surfaces. Both threefold and twofold sites are included in our analysis of methanolic species on the (111) surface.

3. Computational details

The extended Hückel tight binding method has been used to analyze the interactions of oxygen, carbon monoxide and methanol with the (100) and (111) surfaces of TiC. Because of similarities in bonding, structure and reactivity the discussion is restricted to TiC, though actually representative calculations were also done for NbC. These indicated little difference from TiC.

The surface for either face was modeled by a two-dimensional slab of finite thickness [17]. For TiC(100) the slab was three layers deep, while six layers of alternating metal and carbon atoms comprised the TiC(111) model. The final carbon layer of the (111) slab was terminated by hydrogen. This helped to satisfy the valency of the terminal carbon. In certain instances, where the hydrogen was excluded from the calculation, sizeable and unreasonable charge transfer occurred from the bottom-most layer of the slab to the adsorbate molecule. The hydrogenation of the terminal carbon layer did not affect the charge distribution or the overlap population in the surface layer(s), nor did it affect the total charge transfer to the adsorbate.

The input parameters for this study were taken from previous studies on CO on various metal surfaces [18]. These values are given in table 2.

For the sites considered in the theoretical analysis of TiC depicted in fig. 1, the Ti–C nearest neighbor distances are 2.164 Å and the Ti–Ti and C–C face diagonal distances or next nearest neighbor distances are 3.06 Å.

3.1. Clean surfaces

Calculations were performed on both the three-dimensional solid and the two-dimensional surface models. The inclusion of computations on the solid allows for a discussion of the bonding in the substrate and an analysis of the

perturbation of cleavage. Also, such a comparison provides for a test of the model. The bulk layer(s) of the material should be perturbed little by the cleavage that forms the surface, hence bonding in the bulk layer should be similar to that in the three-dimensional solid.

For TiC, the bonding results from a mixture of components: ionic, covalent and metallic. The extent to which each contributes to the bonding has been a topic of debate. In particular, controversy as to the ionic or covalent nature of the material is widespread. Schwarz et al. [19,20] have suggested that the bonding in carbides is covalent, but as one progresses toward oxygen among carbides, nitrides and oxides, the bonding between metal and nonmetal becomes more ionic. Other authors have contended that the bonding in all carbides, nitrides and oxides is primarily ionic [21]. Wijeyesekera and Hoffmann have suggested that the main cohesive factor is covalent bonding between metal and nonmetal atoms [22]. The short metal–metal separations clearly indicate metal–metal bonding is essential in these compounds. Samonov et al. have proposed that the interstitial carbon atoms donate electron density into metal–metal bonding orbital [23]. Though the M–C bond is described as covalent, Schwarz suggests that carbides show the greatest effective charge transfer or polarization of charge between the metal and nonmetal. In the case of the nitrides and oxides the polarization of charge is not as exaggerated. Kim et al. support the conclusions of Schwarz et al. in their suggestion that the ionic character of the metal–nonmetal bond increases from carbon to oxygen [24]. We suspect that there is room for both covalent and ionic descriptions of the carbide bond.

There have been several theoretical studies on the surface electronic structure for TiC(100) and surface states, but few consider facial reactivity and chemisorption [25].

Fig. 2 shows our calculated density of states (DOS) for TiC and the metal contribution to the DOS. What is not on metal is on carbon. The general characteristics of the bands, in order of increasing energy, is obviously, C 2s (-18 to -21 eV), C 2p (-9 to -12 eV), then Ti 3d. The covalent nature of the bonding is manifested by the significant penetration of the metal d levels into the carbon p block. This was found also by Schwarz et al. in the DOS calculated by self-consistent field (SCF) methods (see chapter 2 of ref. [19]). We get a lower density of states at the Fermi level – this results from the choice of parameters in our calculations. Shown in fig. 2, as well, are DOS plots calculated with the APW method of Schwarz and photoelectron spectra for TiC. These provide comparison between experimental and more sophisticated theoretical treatment with the results obtained from our qualitative computations. What is obvious from this comparison is that the features of the photoelectron spectra and the APW calculations are accurately reproduced by our qualitative treatment [26].

We next proceed to model two surfaces, TiC(100), (111). These were shown

in schemes 2 and 3, respectively. The details of the model slab were given in the text above. The decomposition of the DOS into specific Ti and C contributions for the surface layer of TiC(100) is shown in fig. 3. Detailed differences may be gleaned from table 3, which also gives for comparison some indicators of the bonding in bulk TiC. The following observations may be made.

(a) The total DOS curves are similar for the bulk and the slab model, as they should be. There is a somewhat greater band gap at the Fermi level in the surface model.

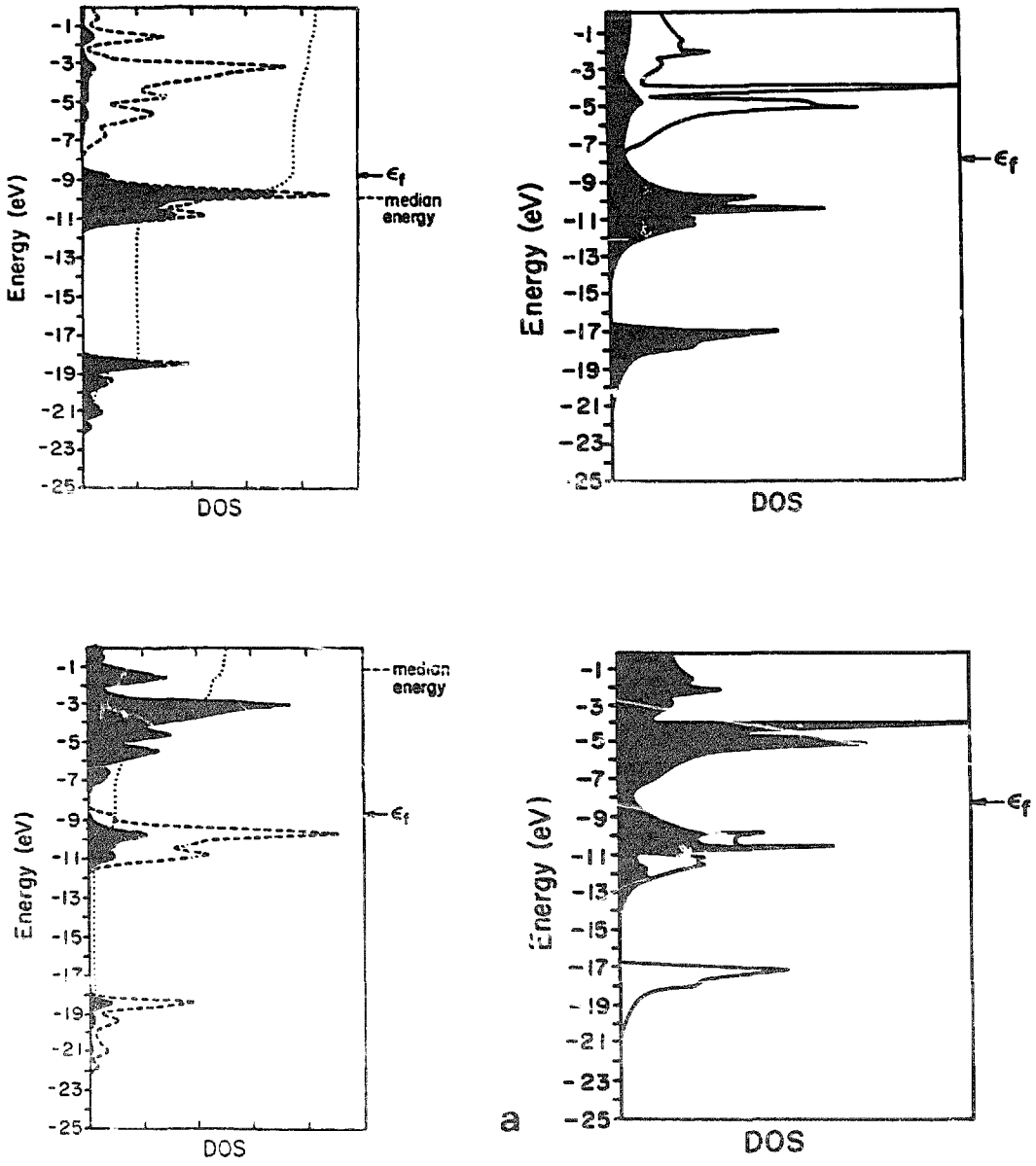

Fig. 2. Projections of the carbon and titanium atoms for the three-dimensional TiC from EH and APW calculations. Experimental photoelectron spectrum for TiC.

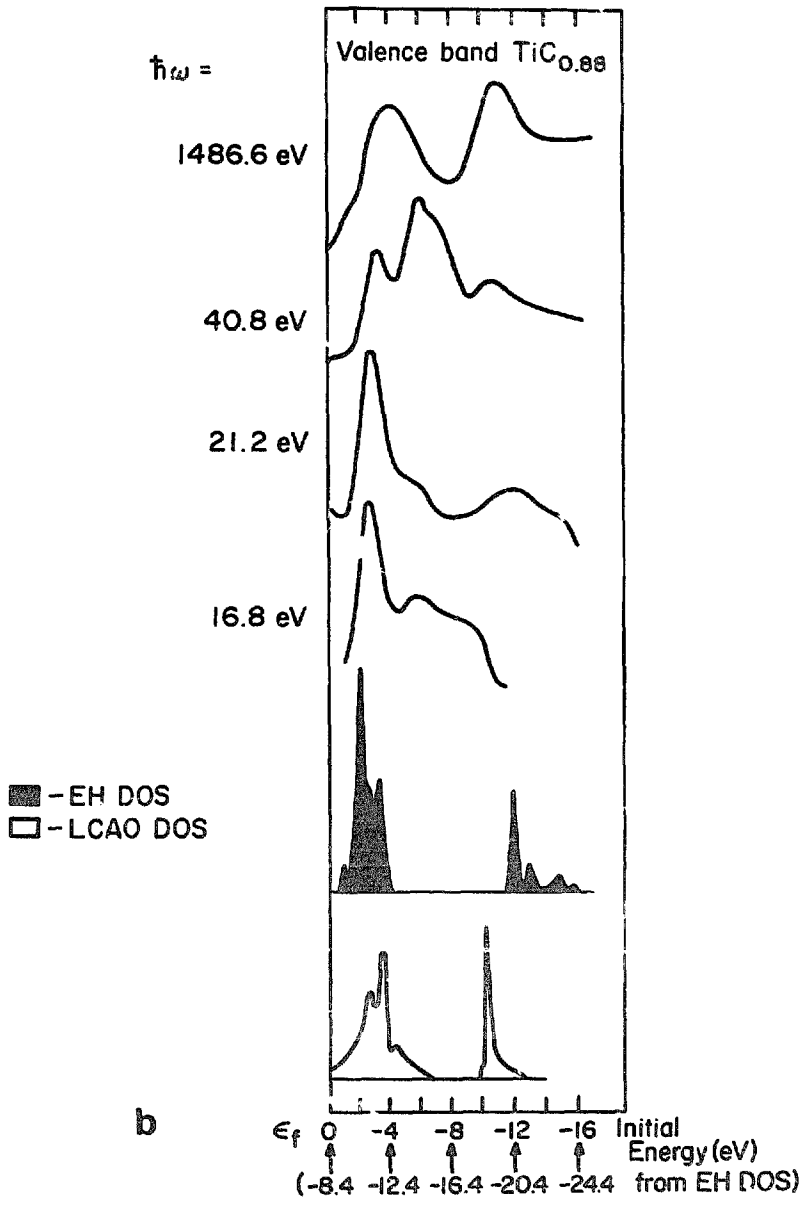

Fig. 2. Continued.

σ in plane bonding, pdσ π bonding (in xy plane) pdπ

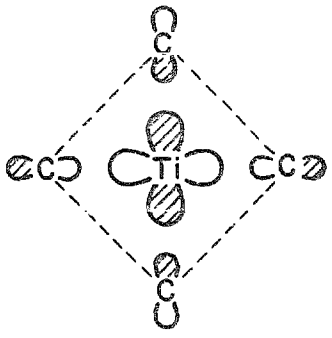

Scheme 5.

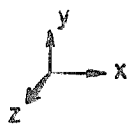

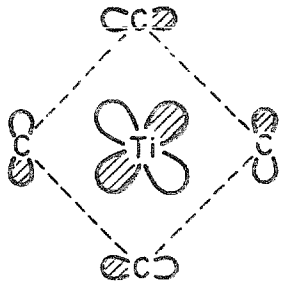

Scheme 6.

(b) There is a significant reduction in electron density on the surface metal atoms. This comes about as a result of cleaving the metal–carbon bonds. The Ti levels are populated as a result of their admixture with C orbitals. Some

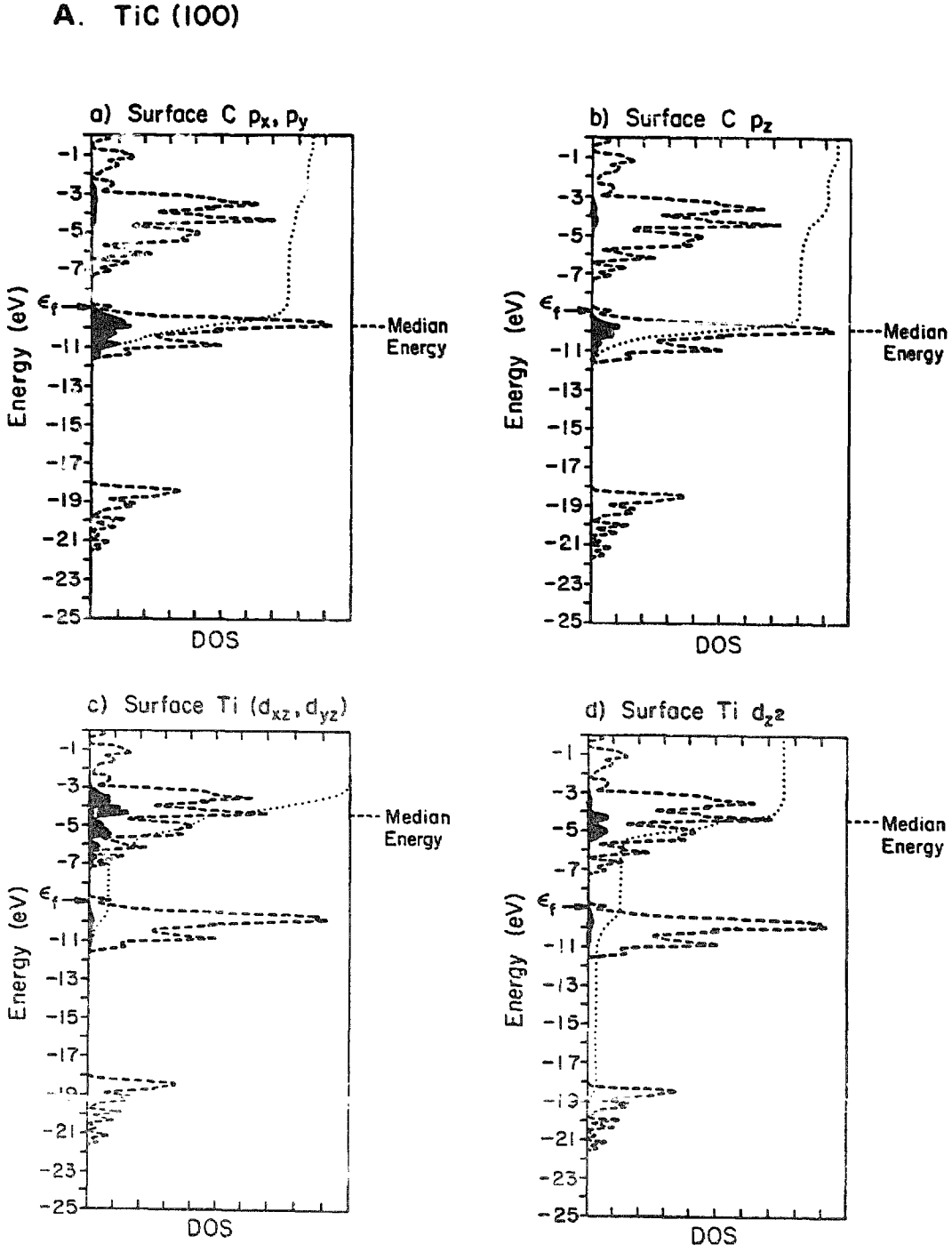

Fig. 3. Atomic orbital contributions of C p and Ti d orbitals to the total DOS of a slab model for the (100) and (111) faces of TiC. The orbital correlation diagram shows the states affected upon surface cleavage.

B. TiC (111)

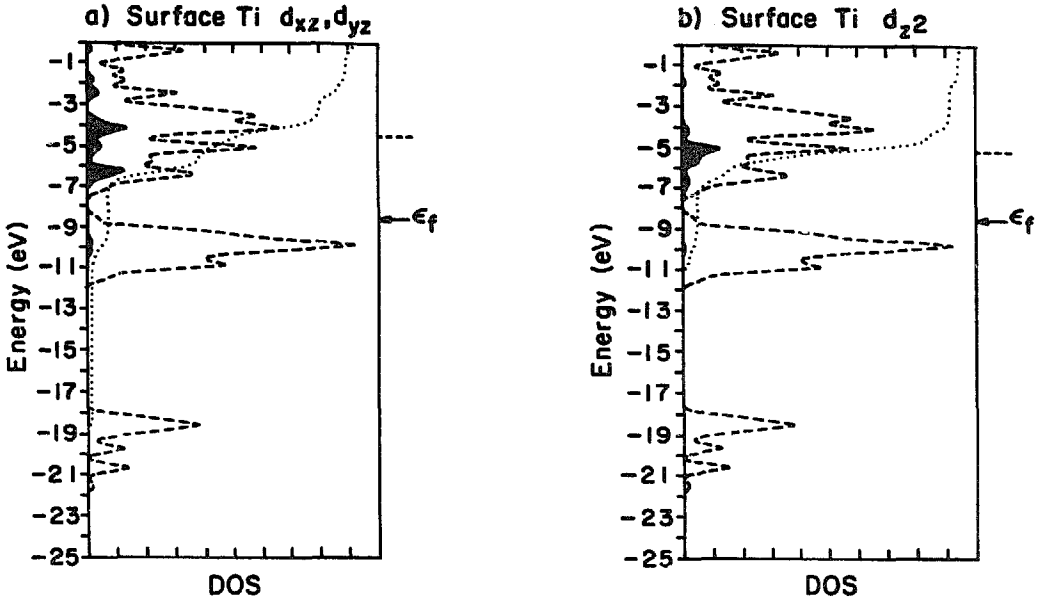

Fig. 3. Continued.

typical local bonding combinations are shown in schemes 5 and 6. The fewer carbon neighbors, the less Ti–C bonding, with its corollary fractional occupation of Ti 3d orbitals. On the different faces, the more Ti–C links that are cleaved in making the surface, the less electron density on Ti.

(c) In general, the substrate carbons are electron-rich. This comes about from the relative electronegativity of the atoms, C > Ti. That the formal charge on C is not 4^- derives from the covalent interactions which push above, the Fermi level, some Ti–C antibonding orbitals. These are analogous to schemes 5 and 6, but with a node between the metal and carbon.

(d) The overlap populations show some enhancement of the bonding at

Table 3
Some characteristics of the bonding in bulk TiC and several TiC surfaces

	Bulk TiC	TiC(100)	TiC(111)	Ti(0001)
Charge				
On (surface) Ti	+2.187	+2.222	+2.454	+0.116
C	−2.186	−2.256	−2.066	–
Overlap population				
Ti–C (surface)	0.388	0.441	–	–
Ti–C (surface–bulk ave.)		0.401	0.409	
Ti–C (bulk)		0.377	–	
Ti–Ti (surface)	0.029	–	0.052	0.335
Ti–Ti (bulk)		–	0.028	0.310

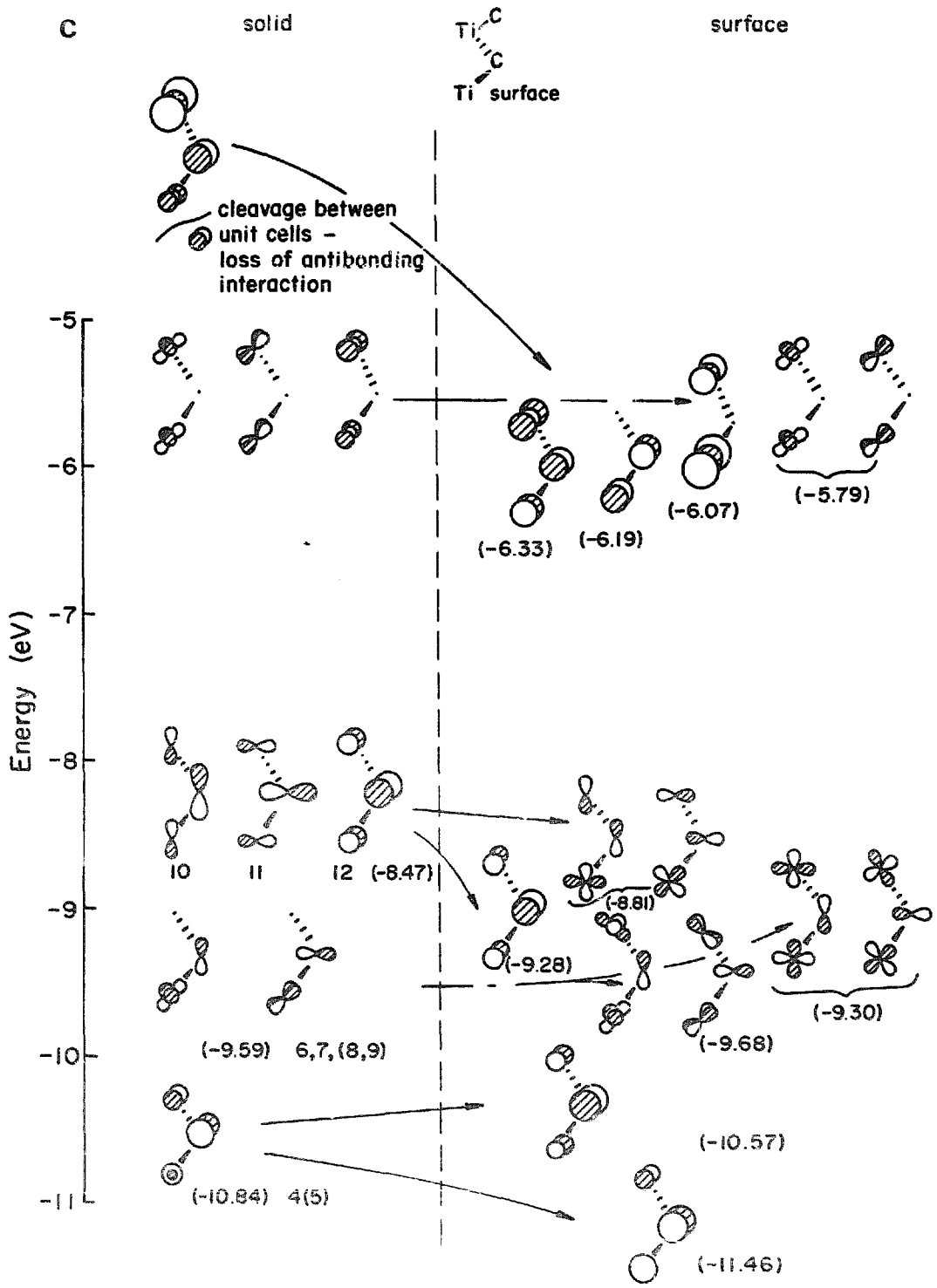

Fig. 3. Continued.

and near the surface. Perhaps one could think of this as electronic relaxation to "heal" broken surface bonds, some electrons normally involved in metal to carbon bonding now being available [27]. One way this is manifested in transition metal surfaces is in a contraction of the surface, e.g. the formation of stronger metal–metal bonds. Some evidence for reconstruction is observed in the case of TaC(100). For this surface there is a contraction between metal and carbon atoms of the surface and bulk layers. This leads to a rippling of the surface in which the surface metal atoms move nearer the bulk atoms and the surface carbon atoms are pushed up slightly relative to the original surface plane. The displacement for the metal is about 4.8% and for the carbon, 4.2%. This gives a total displacement of about 0.2 Å [28].

Experimental studies on the (111) face have shown the existence of a surface state [29]. On this surface, the coordination of the metal atom is threefold. This situation is similar for Ti(0001) where the surface metal is also threefold coordinate. For both of these surfaces, the surface states arises from the dangling bonds or orbitals created upon surface cleavage. Experimentally, the surface state is identified as a small peak just below the Fermi level and is suggested to arise from a 3d state. The most significant contribution to the surface state occurs at the Γ point and shows mainly d_{z^2} character [30]. Our calculations at the zone center are consistent with this assignment. The levels most significantly affected upon crystal cleavage are those with z character. In the solid there are several states which fall near the Fermi level. We can reduce the complexity of the orbital combinations by considering the high symmetry case at the zone center. At this point, there are three states at −8.47 eV which arise from bonding combinations of x, y, and z levels. Just above these levels are metal–metal combinations which show little carbon character, still further up are other z combinations which are antibonding at the cleavage site. When the crystal is cleaved the levels are affected significantly. Several states, which in the solid are antibonding between layers, drop in energy. Some slight changes are also observed in the other combinations but clearly the levels most significantly affected by crystal cleavage are those with significant z character. What about the (100) surface? Formally, for this surface, one ligand is removed. Some change is observed in the d_{z^2} metal and p_z state; however, since these states participate in π bonding within the surface plane and because the metal coordination remains high, the effect of cleavage is not as pronounced. The projected density of states for the TiC(111) are shown in fig. 3 along with those for the (100) surface.

The differences discussed above will prove to be important when we bring up molecules to these surfaces.

3.2. CO on TiC(100) and TiC(111)

Our group has had substantial experience with the analysis of interactions of CO with a variety of metal surfaces [18]. These previous studies provide a

baseline for comparison and paradigm for analysis, so we will begin with this particular chemisorption process.

3.2.1. CO on TiC(100)

The (100) face of TiC has been shown to be the least reactive face of TiC. This has been attributed to the presence of surface carbide and the number of dangling or available bonding orbitals per surface atom provided by surface preparation. Studies on NbC have shown that CO can dissociate at this surface, suggesting significant population of antibonding $2\pi^*$ orbitals of the adsorbed CO [6]. (The two important valence orbitals of CO, 5σ and $2\pi^*$, are sketched in scheme 7 and 8, respectively.) The dissociative sites are proposed to result from carbon vacancies at the surface. Our analysis of CO on this surface includes consideration of vacancy sites. For this study, the CO is presumed to occupy an on top titanium site and the surface coverage considered is 1/2 with respect to surface titanium atoms, i.e., there is one CO molecule for each two titanium surface atoms. This provides for an overall coverage of 1/4 for the "perfect" surface and an adsorbate–adsorbate separation of 4.328 Å for any surface considered. This distance insures that no adsorbate–adsorbate interaction complicates the analysis of the surface–adsorbate chemistry.

In any CO chemisorption (or molecular bonding) the two most important interactions are:

(a) Donation from the 5σ orbital of CO into metal surface orbitals of appropriate symmetry.

(b) Donation from the metal orbitals of appropriate symmetry into the $2\pi^*$ orbitals of CO.

The former process can occur without substantial disruption of the C–O bond, whereas the latter process contributes to weakening of the C–O bond while strengthening the metal–carbon bond. The orbitals typically involved in interaction with the 5σ and $2\pi^*$ orbitals of the CO are d_{z^2} and the d_{xz} and d_{yz} pair on the metal. For "pristine" transition metal surfaces this interaction can be traced through the resonances observed in plots of the projected density of states for metal orbitals and pertinent adsorbate orbitals. These projections can then be compared with the COOP curves to suggest the nature

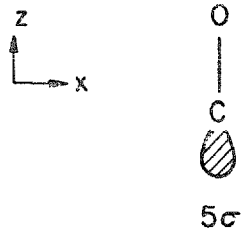

Scheme 7.

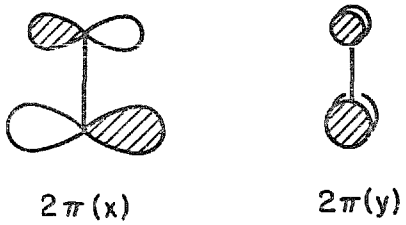

Scheme 8.

Table 4
Pertinent overlap populations, occupations and median energies of "CO" FMO orbitals for CO on TiC(100) and TiC(111)

	TiC(100)	$TiC(100)_{0.5}$ [a]	$TiC(100)_0$ [a]	TiC(111)	Ti(0001)
FMO occupations					
5σ	1.731	1.725	1.725	1.727	1.730
$2\pi^*$/orbital	0.132	1.380	1.530	1.430	1.610
Median energy					
$2\pi^*$ (eV)	−7.775	−7.875	−8.275	−7.925	−7.725
Overlap populations					
C–O	1.173	0.437	0.473	0.469	0.430
M–C	0.616	0.976	1.060	1.053	1.110

[a] Subscripts indicate the fraction of carbon at the surface, 0.5 indicates there is one surface carbon for each two titanium surface atoms.

of this interaction. For TiC surfaces, this decomposition is complicated by the additional dispersion in these orbitals provided by interaction with substrate carbon.

When CO is adsorbed on a "perfect" crystalline TiC(100) surface, there is no significant population of the $2\pi^*$ orbitals of CO; correspondingly, there is no significant reduction in the overlap population of the C–O bond. The relevant numbers may be seen in table 4, the decomposition of the DOS in fig. 4.

Two new peaks appear in the DOS of the composite TiC(100) + CO. One is the 5σ of CO appearing with our parameters below the TiC 2p band, the other the $2\pi^*$ of CO, falling in-between the C 2p and Ti 3d bands. Resonances are observed between orbitals that interact. Carbon monoxide 5σ interacts with Ti z^2, s and z (see integration in fig. 4, which shows both the dispersion of the states and the occupation as a function of energy) but most of the z^2 density is above the energy window displayed. The Ti–C bonding in TiC has pushed z^2 to high energy – this is just the local crystal field at work, the same effect that produces the classical t_{2g} below e_g splitting in an octahedral molecular complex. Notice that the integration of the z^2 contribution indicates mixing with a σ orbital lower than 5σ of CO as well.

There are resonances between the $2\pi^*$ level of CO and xz, yz on the metal. But since effectively both of these orbitals are empty, the only occupation of CO $2\pi^*$ that occurs is through the Ti part of the carbon 2p band. And that is small. The perfect TiC surface does not interact well with CO $2\pi^*$, and does not weaken the CO bond much.

The adsorption of CO on TiC(100) in which carbon vacancies activate the surface has also been considered. It is first necessary to consider the influence of the defect on the properties of the clean surface. For this study, the

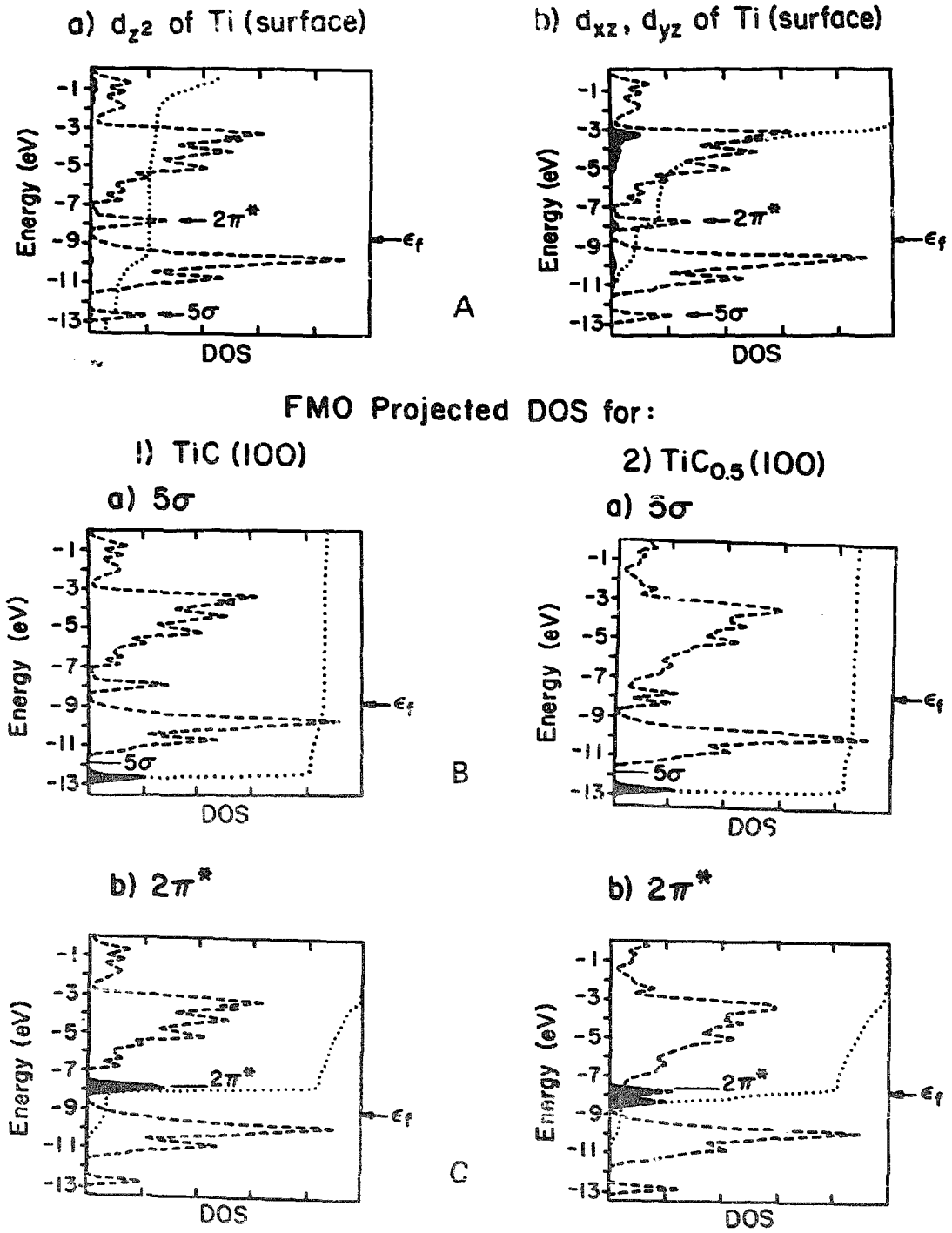

Fig. 4. Projected density of state for: (A) titanium d_{z^2} and $d_{xz,yz}$ orbitals for TiC(100). (B) 5σ CO orbitals on TiC(100) and $TiC_{0.5}$(100). (C) $2\pi^*$ CO orbitals on TiC(100) and $TiC_{0.5}$(100).

percentage of carbon relative to titanium at the surface was chosen to be 100% for the case of the "perfect" surface, 50% and 0%. These concentrations of surface carbon are not suggested to be realistic but should span the range of defects in the "imperfect" TiC lattice. In general, two effects are observed as the surface concentration of carbon decreases. The first is an overall increase in bonding between the affected titanium atom and neighboring atoms. Some Ti orbitals are "freed" from interaction with the carbon removed, come down in energy, and are available for bonding. A second effect is a slight local shift of the Fermi level at the surface to higher energy. Some primarily metal levels, in the Ti 3d band, become occupied on C depletion. This is nothing unusual, it is just a consequence of the electronegativity of Ti and C. The energy of the orbitals removed when a carbon leaves is such that in the solid, were the carbon still there, it would be closer to C^{4-} than C^0. But it is removed as

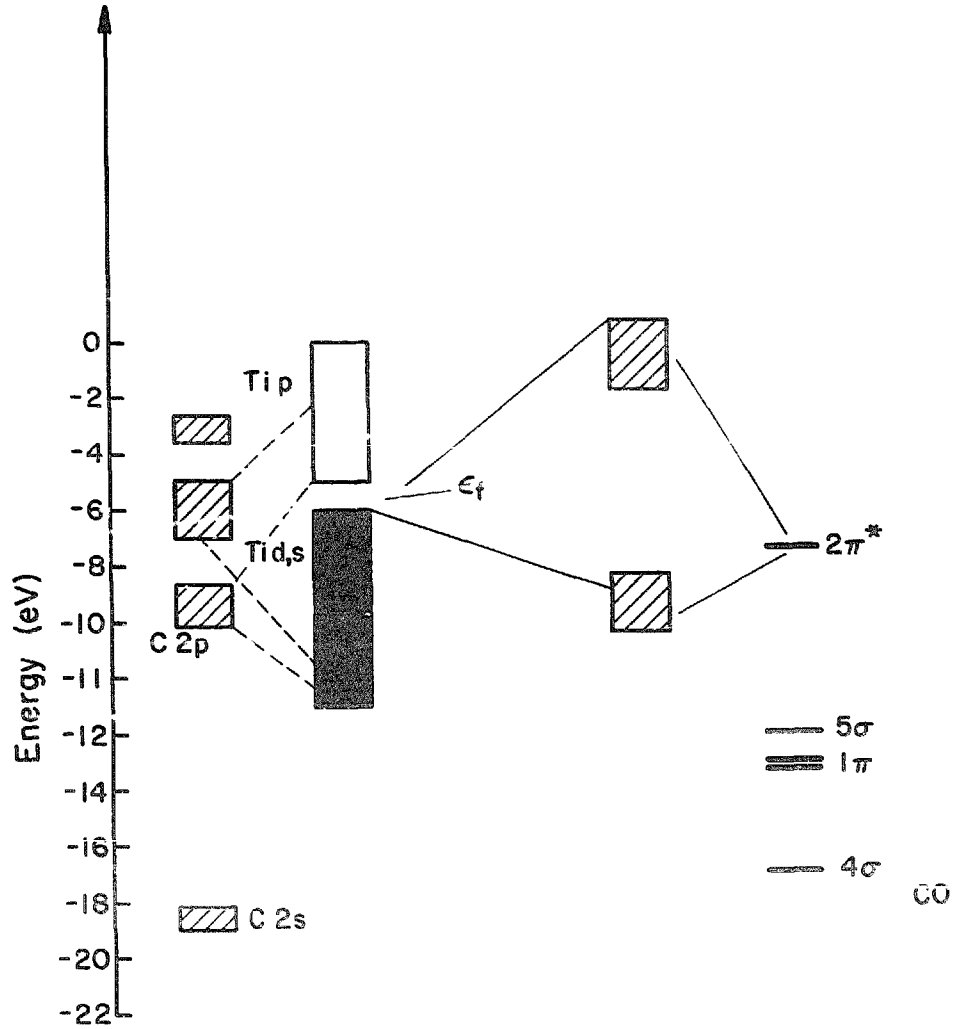

Fig. 5. Schematic showing the motivation for the reduction of the median energy of the $2\pi^*$ levels of CO upon interaction with the TiC surface.

neutral C. The net effect is a reduction of some Ti atoms, a partial filling of the Ti 3d band.

The most significant computed effect of removing surface carbon is activation of the surface. The projected DOS of CO and metal d_{xz}, d_{yz} and d_{z^2} orbitals show many similarities to those of the perfect surface. However, charge transfer from the substrate into the $2\pi^*$ orbital is facilitated in the carbon deficient surface by the increased electron density and the higher energy of the relevant electrons of the bonded titanium atoms. The increased interaction can be followed by the population of the $2\pi^*$ levels of CO, the metal to carbon overlap population or the dispersion of the FMO's of CO. For the TiC(100) surface studies, the median energy of the $2\pi^*$ level decreases as carbon vacancies are formed at the surface. For CO on a transition metal surface, these orbitals are normally pushed up to higher energies as they interact with orbitals of metal d-orbitals of lower energy. But for the carbides, the metal d-block median energy is considerably higher than the $2\pi^*$ levels of CO, and hence this interaction tends to lower the median energy of the CO orbitals and raise the median energy of titanium d-block. This "inverse crystal field" effect is shown schematically in fig. 5. For the "activated" surfaces discussed, the result of creating carbon vacancies at the surface is an increased population of the $2\pi^*$ orbitals of CO and a corresponding increase in the metal–carbon overlap population. The FMO occupations, pertinent overlap populations and median energies of the $2\pi^*$ orbitals are collected in table 4 along with the values from the "perfect" (100) surface.

3.2.2. CO on TiC(111)

The (111) face of the rock salt carbides show reactivity which parallels that of the pristine transition metal surface. For a Ti(0001) surface, CO is dissociatively adsorbed [8]. EH calculations show a large population in the $2\pi^*$ fragment orbitals of the CO, with a correspondingly large metal–carbon overlap population [18]. Calculations on the (111) face of TiC show many similarities to that of Ti(0001). The overlap populations of the C–O and Ti–C (ad-CO) bonds are nearly identical to those obtained from calculations on the pristine metal surface. Also, the general appearance of the projected fragment metal orbitals and COOP curves are quite similar, though the dispersion of the FMO levels is somewhat greater for CO on Ti(0001). The (111) surface of TiC displays a slightly reduced reactivity toward CO, which is manifested in weaker metal–carbon and stronger carbon–oxygen bonding. The apparent similarities between Ti(0001) and TiC(111) are the result of two factors. The first is the symmetry of the adsorbate and substrate. For on-top adsorption, threefold symmetry is preserved for both surfaces. The second consideration is based upon the strength of interaction between adsorbate and substrate. In the case of CO on TiC(100), there was little dispersion obvious in the 5σ and $2\pi^*$ levels of CO. For the (111) surface, however, the dispersion in these levels (the

DOS decompositions are not shown here) is substantially greater.

The interaction of CO with these two surfaces provides some insight as to the role surface carbide plays in the deactivation of the surface. For the (100) face, both the coordination of the surface atoms and presence of surface carbide serves to deactivate the surface. For the perfect (100) surface, we observed no driving force for CO dissociation. Unsaturation increases at the metal atom, and the dispersion observed as a result of the strong covalent bonding between metal and carbon atoms is reduced. This brings the median energy of the implicated surface metal d-orbitals down to a more "reactive" range. The deactivation in this face occurs as a result of the strong covalent interactions of the metal and carbon as well as the coordination sphere of the surface atoms. For the (111) surface, the metal surface atoms are significantly more "unsaturated" in terms of bonding interactions, as many metal–carbon bonds are broken upon surface preparation. This surface is more reactive as the coordination of the surface atoms, in particular the coordination of the metal atoms, with substrate carbide is reduced relative to the (100) face. Such differing reactivities become even more apparent when considering the reaction of methanol with these two surfaces.

3.3. Methanol on TiC(100) and TiC(111)

3.3.1. Oxygen on TiC(100) and TiC(111)

Consideration of the adsorption properties of oxygen on these surfaces is a starting point for studies of methanol on these surfaces. Previous experimental studies have shown that methanolic species interact primarily through their lone-pair orbitals and such adsorbates choose adsorption geometries similar if not identical to that of atomic oxygen.

For TiC(100), ISS experiments performed as a function of oxygen dosage have shown severe attenuation of the carbon 1s signal, while no significant reduction was observed in the intensity of the titanium core levels in surface oxidation studies. These experiments coupled with measurements of the surface dipole discussed previously have suggested that the primary site of interaction is one in which the oxygen sits atop a surface carbon atom [38]. Further, UPS and XPS studies have shown significant changes in the 2s, 2p and 1s orbitals of carbon, respectively, while only slight changes are associated with the titanium levels, suggesting the primary interactions between the substrate and adsorbate are between surface carbon and oxygen [31]. The sites which implicate titanium surface atoms are suggested to be the most unfavorable toward oxygen adsorption.

An interesting question is: How much C–O bonding is there when the O comes on-top of the C. For another point of view is to say that single adatom adsorbates in general prefer hollow sites with high coordination. The site in question is such a fourfold hollow site of the Ti surface lattice. The C–O

overlap calculation we calculate for on-top carbon adsorption of oxygen is 0.468. For a calibration, the value for CO bonds in representative organic molecules is 0.560. Obviously, there is real, substantial CO bonding.

There is also substantial electron transfer toward the oxygen. The charge transfer itself appears to be localized; that is, the primary atoms involved are the adsorbate oxygen and the connected surface carbon atom. This situation provides for minimal disruption of substrate bonding. For oxygen atop a surface titanium atom, the worst possible case for adsorption, an even greater charge transfer is observed. Electron density is lost from almost every atom in the unit cell. These observations suggest two reasons for the site preference. First, the charge transfer or charge polarization is at a relative minimum for the case of on-top carbon adsorption. Secondly, the localized electron transfer preserves bonding within the substrate. Oxygen adsorption on titanium metal and on the polar face of TiC results in a rather large change in the work function. A similar observation is made in the case of oxygen adsorption atop surface titanium. The states contributed by the oxygen do not interact strongly because they are very low in energy. The oxygen 2p states come into the total density of states effectively unperturbed from their atomic position and are filled by transfer from states comprised of orbital components from all atoms in the substrate. This "ionic" interaction is responsible for the sharp unperturbed oxygen levels and is consistent with the large electron transfer. Furthermore, it explains the observation of charge transfer occurring from every atom in the substrate.

For adsorption atop surface carbon, the orbitals involved in "primary" bonding are energetically suited for interaction. Thus greater dispersion is observed for the oxygen 2p orbitals. This dispersion reflects a more covalent bonding situation between the surface carbon and the oxygen and the result of covalent bonding is a modulated and localized charge transfer.

Ideally we should be able to predict the preferred site of adsorption by following oxygen binding energies. In practice we cannot do this because the extended Hückel method does not predict bond distances well. We have to assume Ti–O distances, we cannot optimize them. From our experience charge transfer and the extent of interaction, measured by overlap populations and band dispersions, are better indicators of the quality of bonding.

For the (111) surface, there are two unique adsorption sites for oxygen, one of which is a threefold site, the other is believed to be a twofold site. For TiC(111), there are two possible threefold sites, one in which a carbon lies directly below the surface hollow and another in which there is a "vacancy" directly below the surface hollow. Both of these threefold sites were considered in the EH analysis of oxygen on TiC.

Keeping in mind the limitations of the EH method, the twofold site is calculated to be of lowest energy. The oxygen adsorbed here carries a charge similar to what was observed for oxygen atop carbon on the (100) face. For

Table 5
Pertinent overlap populations and electron density distributions for oxygen on TiC(100) and TiC(111)

	Overlap populations				
	TiC(100) [a]		TiC(111)		
	C–O	Ti–O	2f	3fv [b]	3fc [b]
C–O	0.468	–	0.019	–	−0.020
Ti–O	0.020	0.390	0.298	0.201	0.198
	Electron densities [c]				
	TiC(100) [a]		TiC(111)		
	C on top	Ti on top	2f	3fv [b]	3fc [b]
Ti	1.895	1.764	1.836	1.825	1.868
C	6.587	6.243	–	–	–
O	7.256	7.685	7.247	7.301	7.216

[a] Both sites are on top.
[b] 3fv represents a threefold site in which there is "vacancy" below the surface hollow. 3fc represents the site in which a carbon lies directly below the surface hollow.
[c] For surface Ti, C and adsorbed O.

this site there is a small bonding interaction between the adsorbate atom and the substrate carbon, the magnitude of which is critically dependent on the Ti–O bond distance. The threefold hollow site in which carbon sits directly below the surface hollow is the worst site for adsorption (except for an on-top site) energetically. For this site, the interaction between the substrate carbon and adsorbed oxygen is of approximately the same magnitude as in the case of the bridging oxygen. However, this interaction is antibonding and destabilizes this site toward adsorption. For the other threefold hollow site, the opportunity for stabilization or destabilization through interaction with other substrate atoms does not exist. This site is the second best energetically and shows a larger value for the Ti–O overlap population than does the other threefold site. This suggests that the preferred site is a twofold site, followed by threefold hollow site in which there is no oxygen–carbon interaction possible. The observation of an antibonding relationship between substrate carbide and adsorbed oxygen suggests a mode of deactivation of this surface.

The pertinent overlap populations and charge density distributions are shown in table 5.

3.3.2. Methanol on TiC(100) and TiC(111)

Experimental studies on the adsorption properties of methanol also show the differing degree of reactivity of the two faces prepared. Difference UPS spectra have shown that the O–H bond of the methanol is maintained at the surface for the (100) face of NbC while the UPS spectrum obtained for the

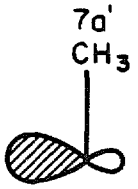

Scheme 9.

Scheme 10.

(111) surface is virtually identical to that obtained for methoxy on nickel and copper surfaces. As far as we know further decomposition of methanol into formaldehyde or related decomposition products has not yet been studied. Let's look at those orbitals of methanol and methoxy likely to interact with a surface. The highest occupied orbitals of methanol are the 7a′ (scheme 9) and 2a″ (scheme 10), both of which are oxygen lone-pair orbitals. It is these two orbitals, especially the higher lying 2a″, which can participate effectively in donor bonding to the surface. The lowest unoccupied orbital, localized on C and O, is too high to interact well. For methoxy there is a similar situation, there is no good acceptor orbital, only the 2e oxygen lone-pair combination, scheme 11. It should be noted that we are thinking about methoxy from an anionic, OCH_3^-, viewpoint, 2e occupied. Alternatively we could take methoxy neutral in which case 2e would be occupied by only three electrons and would serve as both a donor, and as a very good acceptor.

Calculations on the decomposition of methanol on nickel surfaces suggests that methoxy is much more stable at the (100) surface than methanol, though attempts at modeling the decomposition have proved difficult [32]. In a previous paper, we have discussed the interaction of methoxy with Cu(100) and that study has provided a baseline for the calculations of the bonding between methanolic species and the two carbide surfaces of consideration [33].

3.3.2.1. Methanol/methoxy on TiC(100) For the (100) the methanol is proposed to interact primarily with the surface carbon atom through the 7a′ lone-pair oxygen orbital. The UPS spectra for methanol on NbC(100) show that the most significant energetic perturbation is for this particular molecular orbital. Also, UPS and XPS studies show that the energies of the valence and core electrons of the surface carbon are shifted significantly, while there is little affect on those of the surface titanium. Since the main interaction between adsorbate and surface seems only to affect the surface carbon, the

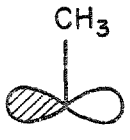

Scheme 11.

a Scheme 12. b

methanol is assumed to be adsorbed through the oxygen, such that the C–O bond vector of the methanol is perpendicular to the plane. Studies of methoxy on other surfaces have shown perpendicular geometries or species which are slightly tilted from the surface normal.

For the (100) surface, the geometry used by us in our calculations is one in which the oxygen of the methanol/methoxy is atop a surface carbon and the C–O bond vector of methanol is perpendicular to the surface plane. In the case of methanol, there remains a degree of freedom for placing the OH bond. There are two sites which should represent the extrema; the first is one in which the hydrogen is directed at a surface titanium and the second directs the hydrogen between two surface titanium atoms, i.e. approaching a bridging position. Both geometries have been considered, however, little difference is computed. The discussion therefore is limited to the second site described in which the hydroxyl proton takes on more realistic orientation given what is known about hydrogen adsorption at surfaces. The adsorption geometries for methanol and methoxy are shown in schemes 12 and 13.

The distance between the surface carbon and methanolic oxygen is chosen as a C–O single bond distance of 1.42 Å. This provides for a relatively short distance between this same surface carbon and the hydroxyl proton and suggests a potential for interaction.

For either rotational extreme, the hydrogen of the methanol does not interact in a significant way with surface titanium.

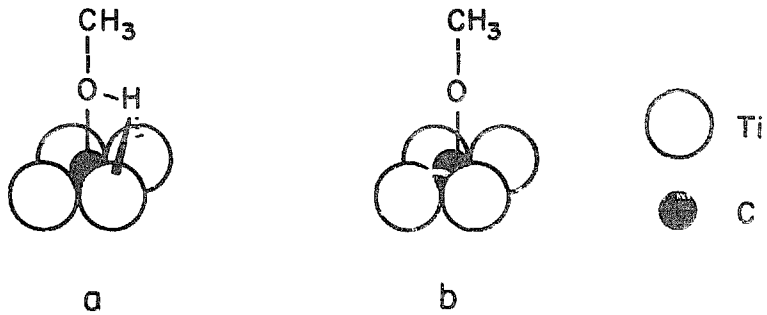

a b

Scheme 13.

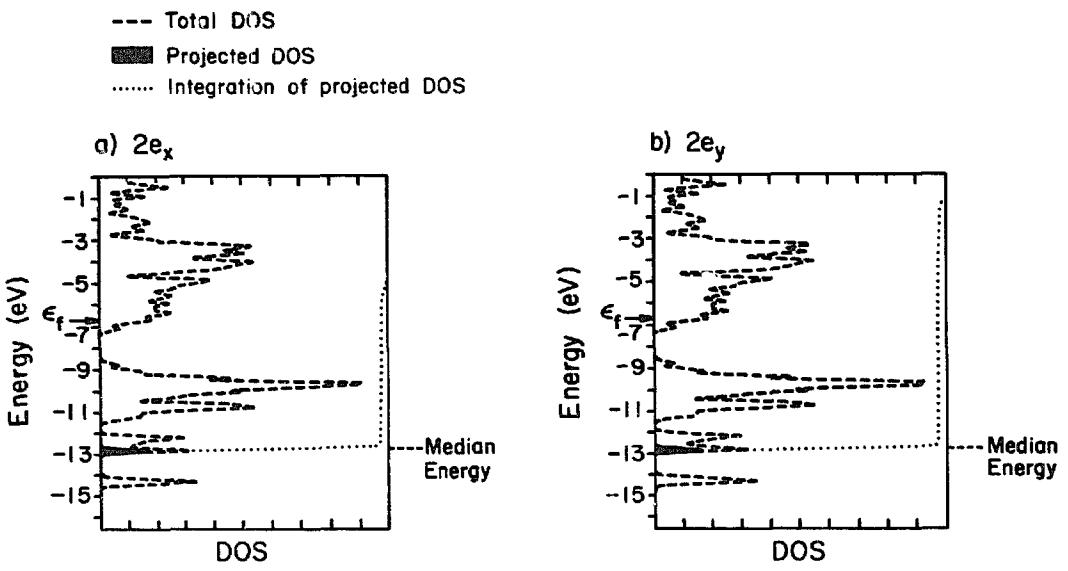

Fig. 6. Projected density of states contributions of 2e orbitals of methoxy on TiC(100).

When one examines the 7a′, 2a″ and 2e contributions to the DOS of the surface–adsorbate complex, one does not see any major differences between methoxy and methanol. One such decomposition for methoxy 2e is shown in fig. 6. Note the position of the 2e way below the Fermi level; we are obviously near the methoxide, OCH_3^-, extreme.

While the DOS curves do not reveal much that differentiates, the overlap population of the surface carbon and methanolic oxygen varies significantly between these adsorbates. In the case of methanol adsorption the C–O overlap population has a value of 0.317 whereas that associated with the adsorption of methoxy is 0.469. The O–H overlap population falls from 0.609 in free methanol to 0.480 at this surface. These observations lead one to expect that the overall binding energy of methoxy should be more favorable than that of methanol. However, the $C_{surface}$–H interaction mentioned previously provides a compensating bonding interaction which seems to stabilize methanol at the surface. Within the accuracy of the EH method there is no energetic preference for either methanol or methoxy at this surface. Though the bonding between the surface and methanol is somewhat complicated by the diversity of orbital types located at the Fermi level, an analogy can be made between the

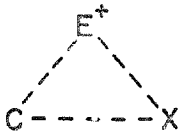

Scheme 14.

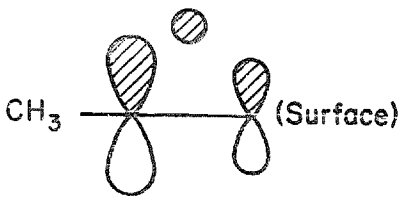

Scheme 15.

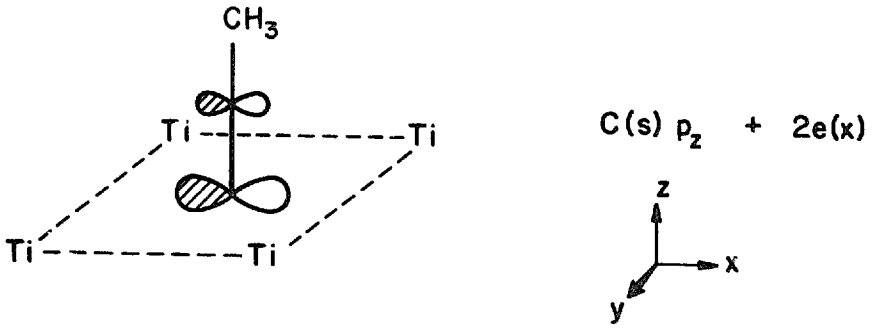

Scheme 16.

bonding observed for molecular methanol and the surface carbon. This explains the formation of the weakly associated three center bonded species and maintenance of the O–H bond.

Normally, three-centered bonding is invoked by the insertion of an electrophile into a C–X bond. In this case, the methanolic proton can be thought of as an electrophile attacking and inserting into the $C_{surface}$–O bond as shown in schemes 14 and 15 below [34].

The interaction of the lone-pair orbitals of either species with the surface provides for surface–adsorbate bonding. Though the dispersion in the 7a′, 2a″ or 2e pair is not large, the median energy of these orbitals reflects the extent to which these donor orbitals interact with the surface. For methanol, the 1a″ orbital is slightly depopulated and its mean energy is lowered by approximately 0.80 eV. A comparison of the projected density of states for these particular orbitals and the COOP curves [35] for C–O bonding in methanol. $C_{surface}$–$O_{methanol}$ and $C_{surface}$–$H_{methanol}$ show that this orbital is affected by interaction of surface carbon with the hydroxyl proton of the methanol. The COOP curves for the $C_{surface}$–$O_{methanol}$ bonding for both adsorbates show significant dispersion in the 2e set or 7a′ and 2a″ levels, though all of the levels of either methanol or methoxy appear to interact in a bonding way with the surface carbon.

How does the oxygen-containing adsorbate bond to the surface carbon? We think the C $2p_z$ interact with methanol orbitals of a′ symmetry or methoxy orbitals of a_1 symmetry, while the a″ and e sets interact primarily with C $2p_x$,p_y orbitals. This is shown in scheme 16. Decompositions of the DOS curves are behind this interpretation.

The carbon-oxygen bond is really quite well formed. This allows us to think of the system in another way, as being generated from the hypothetical surface adsorption of a CH_3OC molecular species. They could be thought of as the iso analogues (as isocyanide is to cyanide) of acetyl species, CH_3CO. These molecules are not well known though have been considered in theoretical studies [36]. The $COCH_3^+$ species has been proposed to be a complex formed

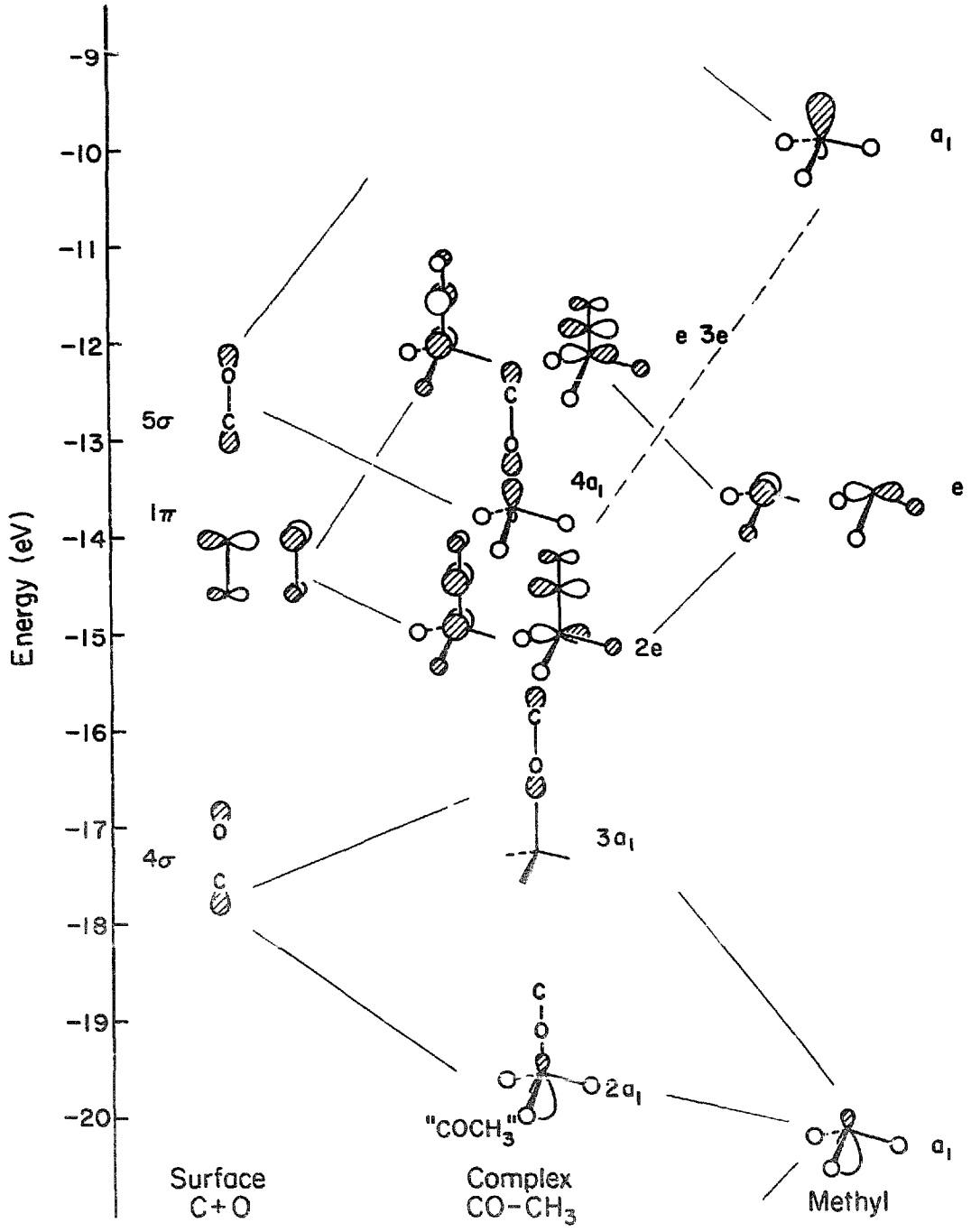

Fig. 7. Orbitals of $COCH_3$ analyzed in terms of CO and CH_3 interaction.

from o-methylation of carbon monoxide. The theoretical study suggests that O–C(CH_3) bond is long, 1.749 Å while the C–O bond is 1.146 Å as in gas phase CO. Fig. 7 shows the orbitals of a hypothetical CH_3OC and Fig. 8 shows some decompositions of the DOS in terms of the FMO's of this molecule and of CO and CH_3 fragments. It appears that this is a reasonable perspective. We

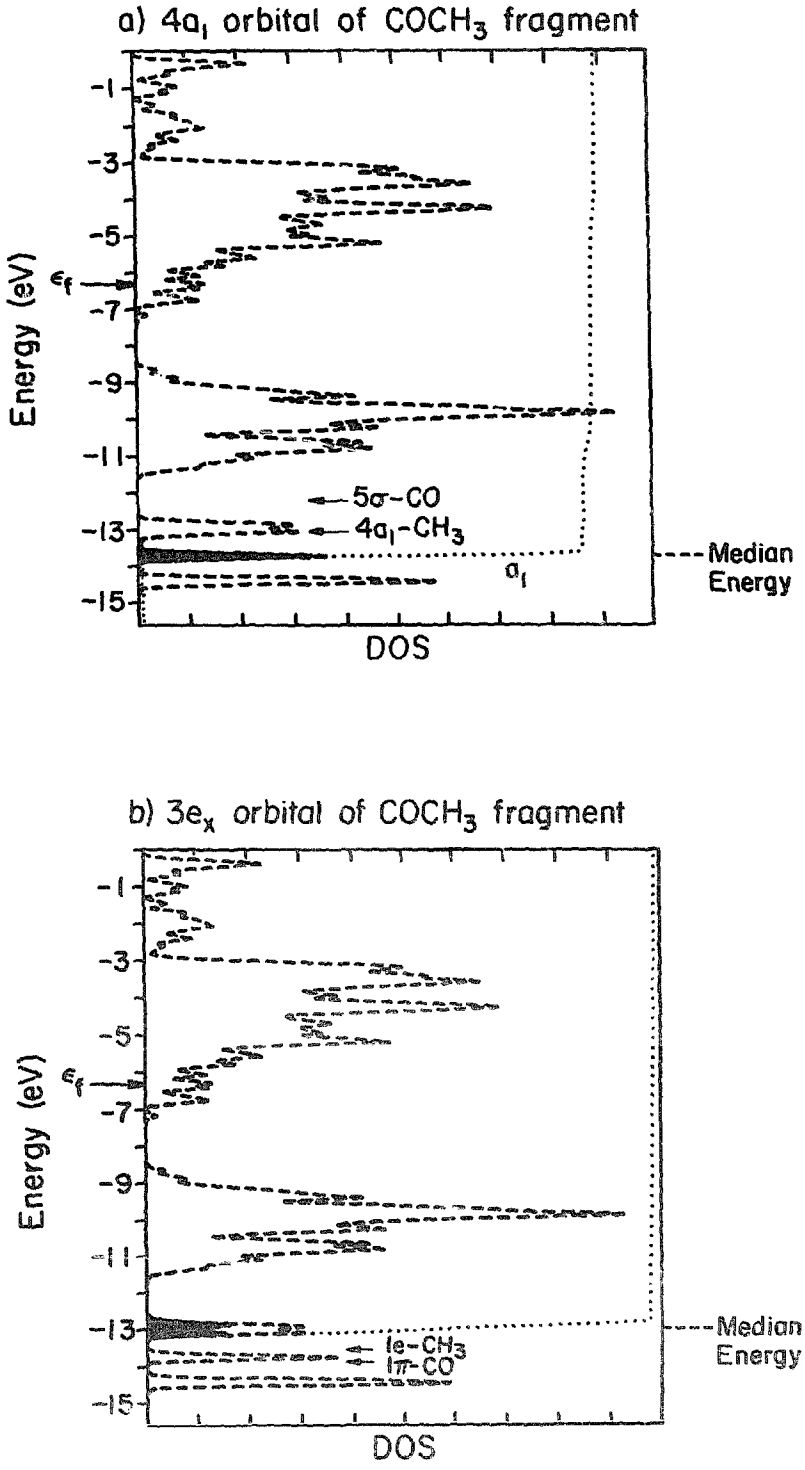

Fig. 8. Projected density of states for fragment orbitals of $COCH_3$.

might note that CH_2OC has π-type orbitals similar to those of CO 1π and $2\pi^*$. These are seen in the DOS of fig. 7 and can be related to our earlier discussion of CO adsorption on C deficient TiC surfaces.

One is also led to think of the fascinating story of secondary metal coordination, at the oxygen end of transition metal carbonyls,

$$L_nM\text{--}C\text{--}O\text{--}M', \tag{3}$$

where L_nM is CH_3 and M′ is surface C of TiC(100), which bear a similarity to the bonding suggested for CH_3O on TiC(100) [37].

3.3.2.2. Methanol/methoxy on TiC(111) For methoxy or methanol on metal surfaces, the adsorption sites which have been proposed assume multiple coordination at the oxygen. Twofold bridging sites are observed when the surface bonds are long, while maximal coordination, in hollows, is observed for shorter surface bond lengths. This is consistent with the observations made for atomic adsorbates. Further, Yates et al. have proposed that the intermediate for methanol decomposition on a Ni(111) surface is one in which the oxygen sits at a twofold site and the methanolic proton is directed at the threefold hollow [16]. For the (111) face of TiC two unique sites are identified for oxygen, one of them representing maximum coordination. The other site is suggested to be a bridging site and the calculations discussed previously have proposed this site to be more energetically favorable. Both sites have been considered in the analysis of methanol and methoxy species at this surface. This discussion will be restricted to the second bridging site as this site is consistent with the site proposed by Yates, and suggested most stable by studies of atomic adsorption on several surfaces. It is proposed to be the most favorable in the theoretical treatment provided above in the discussion of the surface chemistry of TiC.

Yates has suggested that the reaction coordinate for the decomposition of methanol to methoxy is the opening of the COH bond angle, not stretching of the O–H bond [36]. This mechanism was considered as a means of methoxy production on this face. The criterion for O–H bond breakage is normally the magnitude of the overlap population relative to that computed for the free molecule. This angle was varied from 109° to 180° in increments of 10°. No significant reduction was observed in the O–H overlap population relative to that of the free molecule in a similar perturbed geometry. In general, the methodology used to evaluate interactions has been to keep all bond lengths the same and follow changes in the overlap population as a function of changes in adsorption site, coordination or bond angle, as the overlap population is dependent on the bond distance. Using this approach no significant differences were observed in the overlap population associated with O–H bond as a function of increasing COH angle. One really should simultaneously open the bond angle while increasing the O–H bond distance. The combination of these two motions will certainly lead to greater interaction of the hydroxyl proton with the substrate.

Table 6
Charge distribution for methanolic adsorbates on TiC(111)

	Atomic charges				
	Ad-methanol	Free	Ad-methoxy/ad	Free	
				CH_3O^-	CH_3O
O	−0.579	−0.897	−1.011	−1.509	−1.042
C	0.581	0.611	0.595	0.657	0.848
H (methyl)	−0.054	−0.050	−0.056	−0.049	0.063
H (O–H)	0.309	0.436	-	-	-

Two motions were studied in our analysis; the first utilizes the observed O–H bond distance and the second the extreme case of methoxy adsorption. This allows a comparison between the two surfaces of study.

For methanol in this adsorption site, as discussed previously, the primary interactions are between the titanium d_{xz}, d_{yz} and d_{z^2} orbitals and the lone-pair orbitals of the oxygen. The same arguments can be made in terms of the enhanced surface–adsorbate bonding for methoxy over methanol, however for methanol on this surface there are no compensating bonding interactions to provide stability for the surface methanol. For methoxy the degeneracy of the orbitals of e symmetry is broken upon adsorption into this twofold site. This can be seen in projections of the 1e and 2e sets of orbitals. In either case, the dispersion of these orbitals does not appear to be very great and the FMO populations give no indication as to the mechanism of O–H bond breakage or adsorbate–surface bonding. Projections of surface titanium d-orbitals and atomic orbital populations are quite similar for two adsorbates.

Some differences between the two adsorbates are seen in the calculations. First, the charge at the methanolic oxygen is greater in the case of methoxy than methanol. In particular the p_x and p_y orbitals show greater populations for methoxy than for methanol. In either case, there is less electron density at the oxygen than in the case of free methanol or methoxy species. Furthermore, there seems to be little affect on the charges on the carbon or hydrogen atoms of the adsorbate molecules. This is consistent with the UPS experiment that suggests that the lone-pair orbitals of the methanolic adsorbate are those involved in bonding with the surface metal atoms. Table 6 shows a comparison of the adsorbate charge density distribution for methanol/methoxy on the surfaces discussed compared with the charges of the free moieties. In either case, the electron density at the oxygen is much greater for methoxy than for methanol adsorbates. A parallel observation is made for the threefold adsorption site discussed previously. The mode of bonding for methanolic species is similar to that of the 5σ of CO. The lone-pair orbitals are filled and donate to metal orbitals of the appropriate symmetry.

Methoxy is normally not observed as a free reaction product in most studies of methanol/methoxy surface reactions on unaltered metal surfaces. Instead the methoxy and protic species recombine to give molecular methanol as a primary desorption product. For surfaces which have been predosed with oxygen, the adsorbed oxygen atoms react with the methanolic protons and are desorbed as water molecules, while the methoxy species continues to react to give formaldehyde or other decomposition products. Some parallel can be made between the properties of this methoxy adsorbate and adsorbed oxygen. First, the oxygen is a site of enhanced negative charge. The primary interactions between this oxygen atom and the surface orbitals are through oxygen lone-pair orbitals comprised of p_x and p_y orbital components. For atomic oxygen, the bonding situation is similar. The main interactions are between surface metal d_{xz} and d_{yz} orbitals with the p_x and p_y orbitals of the oxygen atom. The EH calculations help provide a rationale for this observation. Adsorption of methanol leads to formation of protic and methoxy species at the surface. The decomposition of the methanol provides for localization of negative charge at the oxygen of the methoxy, which in turn activates this oxygen for recombination with the methanolic protons at the surface. The oxygen of the methoxy behaves as the preadsorbed oxygen.

Calculations on the (111) face of TiC suggest that the bonding between the surface titanium atoms and oxygen atoms of the methanolic species is modified by the presence of the methanolic proton in a manner similar to that of the (100) face. For methoxy a stronger overlap population is observed for the $Ti_{surface}$–O bond than in the case of methanol adsorption, but the difference between the Ti–O populations for both adsorbates is quite substantial as the oxygen is multiply coordinate at the surface. The pertinent overlap populations are shown in table 7.

Table 7
Overlap populations for methanol/methoxy on TiC(111) and TiC(100)

Bond	Overlap population				
	Reference [a]	TiC(100)		TiC(111)	
		Methanol	Methoxy	Methanol	Methoxy
C_s–O	0.560	0.318	0.472	–	–
Ti_s–O	0.268	−0.012	−0.014	0.212	0.323
C_{sub}–O		–	–	−0.020	0.013
C_m–O_m	0.561	0.542	0.548	0.558	0.562
O_m–H_m	0.600	0.609	–	0.481	–
C_m–H_m	0.784	0.784	0.784	0.797	0.786
C_s–H_m		0.180			

[a] The references here are for oxygen adsorption on TiC(100) and TiC(111) and free methanolic species.

From the density of states plot, it is ascertained that the metal orbitals responsible for interacting with the two adsorbates are as expected, d_{z^2}, d_{xz} and d_{yz}, though their mode of interaction differs slightly. A consideration of the Ti–O overlap population and the COOP curve associated with this bonding interaction suggests some slight difference between surface adsorbate bonding for the two methanolic species. First, an immediate observation is that there are no antibonding contributions to Ti–O bonding below the Fermi level for methoxy on this surface, whereas interaction of the oxygen lone pairs of methanol provides a small antibonding component. Also, the $4a_1$ orbital

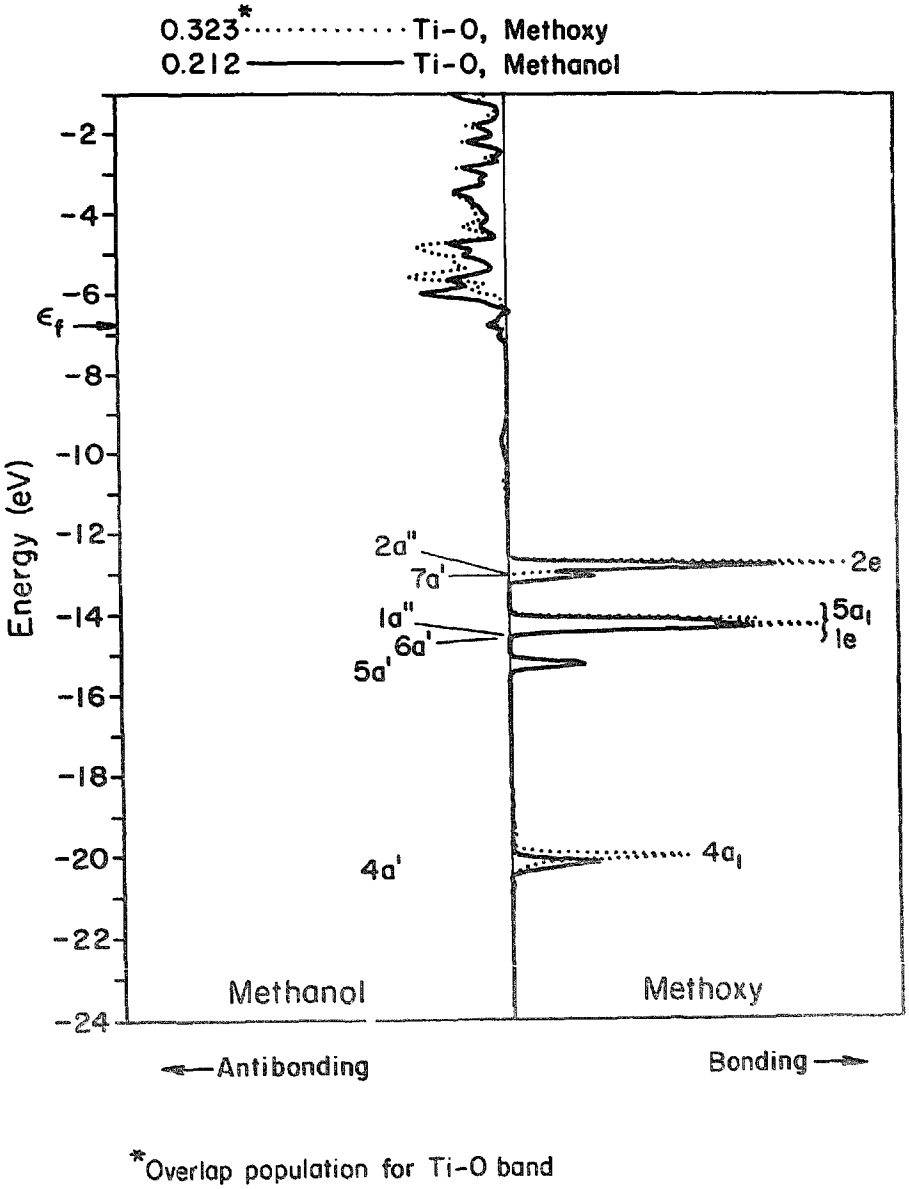

Fig. 9. Comparative COOP curve for Ti–O interaction for methanol and methoxy of TiC(111) and O–H interaction.

seems to be more bonding in the case of methoxy than methanol with respect to underlying Ti levels. In methanol, the corresponding level contributes to O–H bonding and is lowered in energy relative to the titanium d orbitals. There is also some competition between the hydroxyl proton and the surface titanium for the $7a'$ and $2a''$ orbitals of methanol. This can be seen in a comparison of the COOP curves for the Ti–O and the O–H interactions shown in fig. 9.

On this surface there seems to be a competition between the titanium surface and methanolic proton for the oxygen lone-pair orbitals. The preference for methoxy can be traced to energetic and bonding effects. Also, the calculations suggest a rationale for recombination of the methoxy and protic species at the surface.

The EH calculations describe a mode of bonding between the methanolic species and the surface which is consistent with the experimental observation for methanol reactivity on many surfaces. Further, the competition between substrate and protic species is demonstrated for both surfaces. For the (100) surface, the interaction between the surface carbon and methanolic proton modulates the C–O interaction while forming a weakly associated three center system. Such a situation is not possible for the (111) face as both the surface titanium and methanolic proton act as electrophiles and an "exchange" occurs between the methanol proton and the surface titanium atoms. The recombination of methoxy with the hydroxyl proton is also reflected in these calculations. Many similarities between adsorbed oxygen and methoxy are noted. Further, the localized electron density at the oxygen on this surface suggests that a reaction with the hydroxyl proton may lead to formation and desorption of molecular methanol.

4. Conclusions

This analysis of the surface chemistry of the transition metal carbides has provided a description of interactions between adsorbates and surfaces which should be of general use to surface chemists, while demonstrating the additional diversity in reactivity presented by such materials. For the rock salt carbides of this study, the (100) face exposes, for reaction, both metal and nonmetal atoms, whereas the (111) face exposes only transition metal atoms. This provides for diversity in reactivity due to surface composition and structure. Also, the effect of coadsorbed impurities on the surface is addressed in this study. For example, the Blyholder mechanism suggests that electronegative adsorbates tend to reduce the donor properties of the surface and hence reduce the reactivity toward certain adsorbates [38]. The (100) face is proposed as a model for adsorption of a carbon monolayer on an fcc metal whereas the (111) face shows similarities to the reconstructed W(100)-(5 × 1)-C [39].

Acknowledgements

We are grateful to the Office of Naval Research for its support of our work and to Jane Jorgensen and Elisabeth Fields for their expert drawings.

References

[1] For recent reviews on poisoning and promotion see:
G.A. Martin, in: Metal Support and Metal-Additive Effects in Catalysis, Ed. B. Imelik (Elsevier, Amsterdam, 1982);
D.W. Goodman, Role of Promoters and Poisons in CO Hydrogenation, Proc. IUCCP Symp., 1984.
[2] See for example:
L.E. Toth, Transition Metal Carbides and Nitrides (Academic Press, New York, 1971);
P. Swarzkopf, R. Kieffer, W. Leszynski and F. Benesovosky, Refractory Hard Metals (Macmillan, New York, 1953).
[3] A. Neckel, Intern. J. Quantum Chem. 23 (1983) 1317, and references therein.
[4] D.O. Goodman, R.D. Kelly, T.E. Madey and J.T. Yates, Catalysis 63 (1980) 226.
J.A. Rabo, A.P. Risch and M.C. Poutsma, J. Catalysis 53 (1976) 295.
[5] For reactivity of polycrystalline carbides with respect to hydrocarbon synthesis and isomerization and oxidation see:
I. Kojima, E. Miyazaki, Y. Inoue and I. Yasumori, J. Catalysis 59 (1979) 472;
M. Astier, A. Bertrand, S. Teichner, M. Levart and G. Bronoel, Bull. Soc. Chim. France 7 (1980) I-311;
R. Burkl and H. Noller, Monatsh. Chem. 108 (1977) 567;
I. Kojima, E. Miyazaki and I. Yasumori, J. Chem. Soc. Chem. Commun. (1980) 573;
I. Kojima, E. Miyazaki, I. Yasumori and Y. Inoue, Bull. Chem. Soc. Japan 58 (1985) 611;
G. Horz, J. Less-Common Metals 100 (1984) 249.
[6] D.E. Eastman, Solid State Commun. 10 (1972) 933.
[7] I. Kojima, M. Orita, E. Miyazaki and S. Otani, Surface Sci. 160 (1985) 153.
[8] C. Oshima, M. Aono, T. Tanaka, S. Kawai, S. Zaime and Y. Shibata, Surface Sci. 102 (1981) 312.
[9] S. Zaima, Y. Shibata, H. Adachi, C. Oshima, S. Otani, M. Aono and Y. Ishizawa, Surface Sci. 157 (1985) 380.
[10] C. Oshima, T. Tanaka, M. Aono, R. Nishitani, S. Kawai and F. Yajima, Appl. Phys. Letters 35 (1980) 822.
[11] H. Plaenitz, M. Scholz and G. Wieghardt, Neue Hütte 28 (1974) 287;
G. Wieghardt, H. Plaenitz and M. Scholz, Technik 30 (1970) 451.
[12] C. Herring, in: Structure and Properties of Solid Surfaces, Ed. R. Gomer (University of Chicago Press, Chicago, IL, 1953) ch. 1.
[13] J.E. Demuth and H. Ibach, Chem. Phys. Letters 60 (1979) 395.
[14] J.C. Tracy, J.M. Blakely, Surface Sci. 15 (1969) 257;
W. Brearley and N.A. Surplice, Surface Sci. 64 (1977) 372.
[15] V.S. Fomenko, Handbook of Thermionic Properties (Plenum, New York, 1966).
[16] S.M. Gates, J.N. Russell and J.T. Yates, Surface Sci. 146 (1984) 199.
[17] J.-Y. Saillard and R. Hoffmann, J. Am. Chem. Soc. 106 (1984) 2006.
[18] S. Sung and R. Hoffmann, J. Am. Chem. Soc. 107 (1985) 578.
[19] K. Schwarz, Band Structure and Chemical Bonding in Transition Metal Carbides and Nitrides, CRC Crit. Rev. Solid State Mater. Sci. (CRC Press, New York).

[20] P. Blaha, J. Redinger and K. Schwarz, Phys. Rev. B31 (1985) 2316.
[21] P. Blaha, K. Schwarz and J. Redinger, J. Phys. F (Metal Phys.) 15 (1985) 263.
[22] S. Wijeyesekera and R. Hoffmann, Organometallics, 3 (1984) 949.
[23] G.V. Samsonov and Ya.S. Umanskiy, Tverdyye Soyedineniya Tugoplavkikh Metallov, State Sci.-Tech. (Lit. Publ. House, Moscow), for English translation see NASA Tech. Transl. F-102 (1962), and references therein.
[24] S. Kim and R.S. Williams, J. Vacuum Sci. Technol. A4 (1986) 1603;
S. Kim and R.S. Williams, preprint.
[25] E. Wimmer, J. Phys. C (Solid State Phys.) 17 (1984) L365;
E. Wimmer and A. Neckel, Phys. Rev. B31 (1985) 2370.
[26] A.L. Hagstrom and L.I. Johansson, J. Electron Spectrosc. Related Phenomena 11 (1979) 75.
[27] G. Somorjai, Chemistry in Two Dimensions: Surfaces (Cornell University Press, Ithaca, NY, 1981).
[28] J.R. Noonan, J. Vacuum Sci. Technol., in press.
[29] For a discussion of surface states in transition metal carbides and nitrides see ref. [9] and: J. Redinger and P. Weinberger, Phys. Rev. B, in press.
[30] P.J. Feibelman and D.R. Hamann, Solid State Commun. 31 (1979) 413;
P.J. Feibelman, J.A. Applebaum and D.R. Hamann, Phys. Rev. B20 (1979) 1433.
[31] M. Aono, Y. Hou, R. Souda, C. Oshima, S. Otani and Y. Ishizawa, Phys. Rev. Letters 50 (1983) 1293.
[32] T. Upton, J. Vacuum Sci. Technol. 20 (1982) 527.
[33] D. Zeroka and R. Hoffmann, Langmuir 2 (1986) 553.
[34] T.A. Albright, J.K. Burdett and M. Whangbo, Orbital Interactions in Chemistry (Wiley, New York, 1985) pp. 86, 99.
[35] COOP curves are overlap population weighted DOS. They measure the extent of bonding in the solid. For details see refs. [21,33].
[36] R.H. Nobes, W.J. Bouma and L. Radom, J. Am. Chem. Soc. 105 (1983) 309.
[37] C.P. Horwitz and D.F. Shriver, Advan. Organometal. Chem. 23 (1984) 219.
[38] G. Blyholder, J. Chem. Phys. 68 (1964) 2772.
[39] For a description of the carbided tungsten surface see:
J.B. Benzinger, E.I. Ko and R.J. Madix, J. Catalysis 54 (1978) 414;
K.J. Rawlings, S.D. Foulias and B.J. Hopkins, J. Phys. C (Solid State Phys.) 14 (1981) 5411;
P.M. Stefan and W.E. Spicer, Surface Sci. 149 (1985) 423.